ACS APPLIED MATERIALS & INTERFACES

Research Article

www.acsami.org

Surface-Enhanced Raman Scattering-Active Au/SiO_2 Nanocomposites Prepared Using Sonoelectrochemical Pulse Deposition Methods

Chun-Chao Chang,[†,‡,§] Kuang-Hsuan Yang,[⊥] Yu-Chuan Liu,*[,#,§] Ting-Chu Hsu,[∥] and Fu-Der Mai[#,§]

[†]Division of Gastroenterology and Hepatology, Department of Internal Medicine, Taipei Medical University Hospital, No. 250, Wu-Hsing St., Taipei 11031, Taiwan

[‡]Department of Internal Medicine, School of Medicine, College of Medicine, [#]Department of Biochemistry, School of Medicine, College of Medicine, and [§]Biomedical Mass Imaging Research Center, Taipei Medical University, No. 250, Wu-Hsing St., Taipei 11031, Taiwan

[⊥]Department of Materials Science and Engineering and [∥]General Education Center, Vanung University, No. 1, Van Nung Road, Chung-Li City, Taiwan

Supporting Information

ABSTRACT: For improving signals, reproducibility, and stabilities of surface-enhanced Raman scattering (SERS), numerous technologies have recently been reported in the literature. However, the fabrication processes are usually complicated. It is well-known that nanoparticles (NPs) of Au and SiO_2 are SERS active and inactive materials, respectively. In this work, a simple synthesis route based on sonoelectrochemical pulse deposition (SEPD) methods has been developed to synthesize effectively SERS-active Au/SiO_2 nanocomposites (NCs) with an enhancement factor of 5.4×10^8. Experimental results indicate that pH value of solution and addition of SiO_2 NPs before and after oxidation−reduction cycles (ORCs) can significantly influence the corresponding SERS activities. Encouragingly, the SERS of Rhodamine 6G (R6G) adsorbed on the developed Au/SiO_2 NCs exhibits a higher intensity by more than 1 order of magnitude, as compared with that of R6G adsorbed on Au NPs synthesized using the same method. Moreover, this improved SERS activity is successfully verified from the mechanisms of electromagnetic (EM) and chemical (CHEM) enhancements.

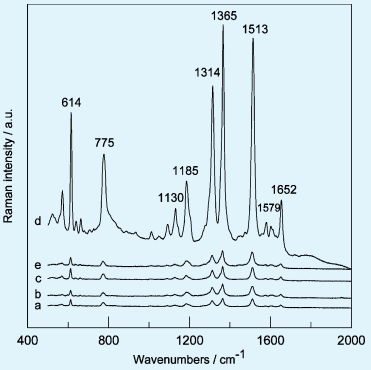

KEYWORDS: *surface-enhanced Raman scattering, mechanisms, electrochemical method, Au/SiO_2 nanocomposites, sonoelectrochemical methods*

INTRODUCTION

Recently, Raman spectroscopy has been popularly used for characterization of famous nanomaterials of carbon nanotube,[1] titania,[2] and graphene.[3] However, the disadvantage is its relatively weak Raman signal from molecules. To resolve this issue technique of surface-enhanced Raman scattering (SERS) was successfully and continuously developed. SERS occurring on rough metal substrates of Ag, Au and Cu is a powerful spectroscopy technique for obtaining vibrational information on adsorbate−surface interactions in view of its unique sensitivity and excellent frequency resolution from the large increase in scattering.[4,5] The generally acceptable mechanism of SERS consists of two major components. One is electromagnetic (EM) enhancement,[6] which results from the enhancement of local electromagnetic fields at the surface of a metal which can support surface plasma/optical conduction resonances. The other is chemical (CHEM) enhancement,[7] which is associated with the charge transfer between the metal and adsorbate at atomic-scale roughness features. In contrast to the well-known EM, the CHEM remains much more enigmatic and hard to ascertain.

In analytical chemistry, signal reproducibility and stability are very important. Therefore, SERS observed on different arrays have been recently developed for its reliable application.[8,9] However, the fabrication processes are relatively laborious. As reported by Zhu et al.,[10] arrays of Au hierarchical micro/nanotowers were achieved on Au-coated silicon planar substrate via electrochemical deposition. The Au hierarchical micro/nanotower arrays have exhibited distinct SERS effect due to the enhanced local electromagnetic field in the vicinity of the sharp nanotips of the towers and the gaps between the neighboring nanotowers. To improve the reproducibility and stability of SERS-active substrates Liao et al.[11] have attempted to develop SERS substrates by the use of two-dimensional (2D) Au nanorod arrays and to characterize the SERS-active sites of the Au nanostructures. They prepared two different types of 2D Au nanorod arrays by means of the anodic aluminum oxide (AAO) template-assisted nanofabrication. The strongest SERS effect was observed for both types of substrates with an Au

Received: June 12, 2012
Accepted: August 30, 2012
Published: August 30, 2012

nanorod diameter of ca. 66 nm. On the other hand, controllable and reproduced surface roughness can be easily generated through control of the electrochemical oxidation−reduction cycles (ORC) procedure.[12,13] Moreover, we have further developed sonoelectrochemical deposition methods to effectively prepare SERS-active metal-island films on substrates. The prepared substrates are more SERS-active and stable.[14,15]

Recently, stable oxides like SiO_2 with low dielectric constant were widely used for synthesizing Au/SiO_2 nanocomposites (NCs) to improve SERS effects.[16−18] Mubeen et al.[16] reported the plasmonic properties of Au nanoparticles (NPs) separated from Au mirror by an ultrathin oxide. The observed SERS intensity is shown to be very sensitive to the dielectric constant of the oxide spacer layer with the most intense signals obtained when using a low dielectric constant oxide layer of SiO_2. Recently, Li et al.[17] reported shell-isolated nanoparticle-enhanced Raman spectroscopy (SHINERS). In their study, thousands of NPs with Au core and an ultrathin SiO_2 shell are spread over a surface. The Au core focuses light and provides Raman signal enhancement by acting as a surface plasmon substrate while the SiO_2 shell prevents the core from interfering with the system under study. Zeng et al.[18] demonstrated that in situ SERS spectroscopy can be used to probe Nafion structure on Au and Pt electrode surfaces. This study is enabled by Au nanoshells overgrown on SiO_2 NPs which provide a very strong Raman enhancement and therefore render superior surface sensitivity. Gerein and Haber[19] reported the effect of ac electrodeposition conditions on the growth of high aspect ratio Cu nanowires in porous aluminum oxide templates. They found that pulsed electrodeposition yielded comparable uniformity of pore-filling and no damage to the porous aluminum oxide templates, even when bulk copper was deposited on them. Since the SERS effects are strongly dependent on the particle size and shape of prepared metal NPs (EM enhancement),[20] and the complexes formed on the metal NPs (CHEM enhancement),[21] in this work, SERS-inactive SiO_2 NPs are incorporated into the deposited SERS-active Au NPs on substrates to synthesize effectively SERS-active Au/SiO_2 NCs by using sonoelectrochemical pulse deposition (SEPD). Effects of pH value of solution and addition of SiO_2 NPs before and after electrochemical oxidation−reduction cycles (ORC) on the corresponding SERS activities are examined from the view points of EM and CHEM enhancements.

EXPERIMENTAL SECTION

Chemical Reagents. Electrolytes of HCl and KCl, and R6G reagents (p.a. grade) purchased from Acros Organics were used as received without further purification. SiO_2 NPs with particle sizes from 10 to 20 nm were purchased from Yong-Zhen technanomaterial Co., Ltd., Taiwan. All of the solutions were prepared using deionized 18.2 MΩ cm water provided from a Milli-Q system.

Preparation of SiO_2- and Au-Containing Complexes in Solution. All the electrochemical experiments were performed in a three-compartment cell at room temperature (22 °C) and were controlled by a potentiostat (model PGSTAT30, Eco Chemie). A sheet of gold with bare surface area of 4 cm^2, a 2 × 4 cm^2 platinum sheet, and KCl-saturated silver−silver chloride (Ag/AgCl) were employed as the working, counter and reference electrodes, respectively. In a typically electrochemical ORCs treatment, the Au electrode was cyclically treated in a deoxygenated 0.1 M KCl aqueous solution containing 1 mM SiO_2 NPs from −0.28 to +1.22 V vs Ag/AgCl at 500 mV/s for 200 scans under slight stirring. The duration at the anodic vertex is 5 s. After the ORC treatment, positively charged Au-adsorbed SiO_2 NPs were formed in the aqueous solution at pH 5.2. Further experimental results indicate that only oxidation operation is difficult to prepare $AuCl_4^-$ ions. Also, it is hard to prepare positively charged Au ions−adsorbed SiO_2 NPs by using direct addition of SiO_2 NPs into the $AuCl_4^-$ solution. For comparison the ORC treatments were also performed in acidic 0.1 M HCl aqueous solutions, and time for the addition of SiO_2 NPs was also changed to after the ORC treatment.

Preparation of SERS-Active Au/SiO_2 NCs on Substrates. Immediately, the Au electrode was replaced by a platinum substrate with a bare surface area of 0.238 cm^2 in the same solution. Here the Pt substrate was chosen because it is inert in the following experiments. Then a cathodic overpotential of 0.6 V and a rest overpotential of 0 V from open circuit potential (OCP) of ca. 0.74 V vs Ag/AgCl was applied in turn under sonication to prepare SERS-active Au/SiO_2 NCs on the Pt substrate. In this electrochemical experiment, the equilibrium potential is the OCP of ca. 0.74 V vs Ag/AgCl. Therefore the applied cathodic potential is 0.14 (0.74−0.6) V vs Ag/AgCl. The ratio of reaction times of cathodic pulse deposition of Au NPs to rest is 0.1. In applying the cathodic overpotential for pulse deposition of Au NPs, the total accumulated deposition time is 60 s for every experiment. The ultrasonic treatment was performed by using an ultrasonic generator (model XL2000, Microson) and operated at 20 kHz with a barium titanate oscillator of 3.2 mm diameter to deliver a power of 80 W. The distance between the barium titanate oscillator rod and the electrode is kept at 5 mm. After this deposition of SERS-active Au/SiO_2 NCs, the Pt substrate was rinsed throughout with deionized water, and finally dried in a dark vacuum-dryer for 1 h at room temperature for subsequent use.

Adsorption of R6G on SERS-Active Au/SiO_2 NCs. For SERS measurements, the prepared SERS-active Au/SiO_2-containing platinum substrates were incubated in 2 × 10^{-6} M R6G aqueous solutions for 30 min. The substrates were then rinsed throughout with deionized water, and finally dried in a dark vacuum-dryer for 1 h at room temperature for subsequent test.

Characterization of SERS-Active Au/SiO_2 NCs on Substrates. Surface morphologies of Au/SiO_2 NCs-containing Pt substrates were examined by scanning electron microscopy (SEM, model S-4700, Hitachi). In high resolution X-ray photoelectron spectroscopy (HRXPS) measurements, a ULVAC PHI Quantera SXM spectrometer with monochromatized Al K_α radiation, 15 kV and 25 W, and an energy resolution of 0.1 eV was used. To avoid the interferential signals from the substrate, an arrangement of tilt 15° geometry between X-ray and samples was used in measurements. To compensate for surface charging effects, all HRXPS spectra are referred to the C 1s neutral carbon peak at 284.8 eV. Surface chemical compositions were determined from peak-area ratios corrected with the approximate instrument sensitivity factors. Raman spectra were obtained (Renishaw InVia Raman spectrometer) by using a confocal microscope employing a diode laser operating at 785 nm with an output power of 1 mW on the sample. A 50×, 0.75 NA Leica objective was used to focus the laser light on the samples. The laser spot size is ca. 2.5 μm^2. A thermoelectrically cooled charge-coupled device (CCD) 1024 × 256 pixels operating at −60 °C was used as the detector with 1 cm^{-1} resolution. All spectra were calibrated with respect to silicon wafer at 520 cm^{-1}. In measurements, a 90° geometry was used to collect the scattered radiation. A holographic notch filter was used to filter the excitation line from the collected light. The acquisition time for each measurement was 10 s. Replicate measurements of five times on different areas were made to verify the spectra were a true representation of each experiment. The relative standard deviation is within 5% based on the strongest band intensity of R6G on the Raman spectrum. Also, different batches of the as synthesized substrates were measured by using the same conditions for three times. The relative deviation from the average value is less than 5% for an individual sample based on the strongest band intensity of R6G on the Raman spectrum.

RESULTS AND DISCUSSION

Characteristics of Au/SiO_2 NCs on Substrates. As shown in our previous study,[22] $AuCl_4^-$ complexes were produced in the chloride-containing solution after the ORC treatment. In this study, SERS-inactive materials of SiO_2 NPs with low dielectric constant were employed to promptly adsorb the produced positively charged Au ions in the anodic scans. Then these positively charged Au ions-adsorbed SiO_2 NPs can be further reduced to controllably synthesize Au/SiO_2 NCs with specific sizes and shapes on Pt substrates by using SEPD methods. Because the molecules located between two metallic NPs display the greatest SERS enhancement,[23,24] this strategy of a fixed cathodic overpotential for Au pulse deposition in shorter time and a rest overpotential for $AuCl_4^-$ complex diffusion in longer time were applied in turn under sonication to prepare effectively SERS-active Au/SiO_2 NCs on the Pt substrates. Moreover, the key point to induce the adsorption of the produced $AuCl_4^-$ or positively charged Au ions onto the surface of SiO_2 NPs is that the pH of the solution should be lower or higher, respectively, than the isoelectric point of the amphoteric SiO_2 (IEP_{SiO2} =2).[25] In this study, a neutral solution of 0.1 M KCl and an acidic solution of 0.1 M HCl were designed for making a difference between their corresponding SERS effects observed on the resulted Au/SiO_2 NCs. After the ORC treatment in 0.1 M KCl solution containing 1 mM SiO_2 NPs the solution pH value of 5.2 was far higher than the IEP_{SiO2} of 2. This is responsible for the effective adsorption of produced positively charged Au ions onto SiO_2 NPs. Then the even incorporation of SiO_2 NPs can work to improve the corresponding SERS performances based on SERS-active Au NPs. On the contrary, after the ORC treatment in 0.1 M HCl solution containing 1 mM SiO_2 NPs the solution pH value of 0.98 was slightly lower than the IEP_{SiO2} of 2. This phenomenon would result in an ineffective adsorption of produced $AuCl_4^-$ onto SiO_2 NPs. Therefore, the surface morphologies of the deposited Au/SiO_2 films on substrates after the subsequent SEPD processes would be different from neutral and acidic solutions.

Figure 1 shows the microstructures of Au NPs-deposited substrates prepared in 0.1 M HCl solutions with and without the addition of 1 mM SiO_2 NPs before the ORC treatment. As shown in Figure 1(a), in the absence of SiO_2 NPs the average particle sizes of the deposited Au NPs are ca. 40 nm. This surface morphology shows a typical aspect of rough surfaces with Raman activity, which demonstrates microstructure smaller than 100 nm.[26,27] In the presence of SiO_2 NPs in preparation the surface morphology of the deposited Au NPs, as shown in Figure 1b, is quite similar with that observed in Figure 1a (in the absence of SiO_2 NPs in preparation), but some aggregated SiO_2 NPs are coating on the deposited Au NPs. This phenomenon is not the desired result of even incorporation of SiO_2 NPs into the Au NPs matrix to significantly change the corresponding surface morphology with strong SERS activity. The reason should be ascribed to the slight different between the solution pH value and the IEP_{SiO2}. Thus SiO_2 NPs and the produced $AuCl_4^-$ complexes after the ORC treatment are individually present in a strong acid solution. Then SiO_2 NPs and the reduced Au NPs from $AuCl_4^-$ cannot be simultaneously deposited on substrate during the following SEPD process.

Figure 2 shows the microstructures of Au NPs-deposited substrates prepared in 0.1 M KCl solutions with and without

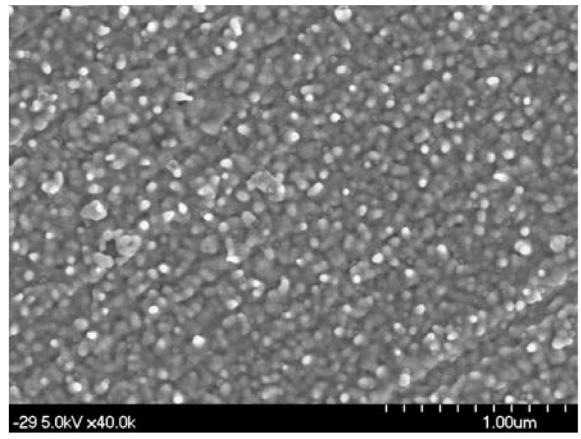

(a)

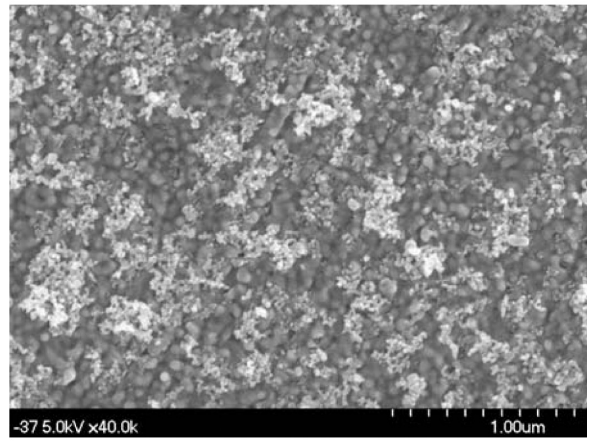

(b)

Figure 1. SEM images of different Au NP-deposited Pt substrates prepared in acidic solutions by using SEPD methods under a cathodic overpotential of 0.6 V and a rest overpotential of 0 V from OCP with a ratio of reaction times of pulse deposition of Au NPs to rest being 0.1: (a) Au NPs prepared in 0.1 M HCl; (b) Au/SiO_2 NCs prepared in 0.1 M HCl containing 1 mM SiO_2 NPs (addition before ORCs).

the addition of 1 mM SiO_2 NPs before and after the ORC treatments. As comparing Figure 2a with Figure 1a, in the absence of SiO_2 NPs the particle sizes and the surface morphologies of deposited Au films are similar, but slightly close packing Au NPs are observed from the KCl solution in preparation. In the addition of SiO_2 NPs after the ORC treatment the surface morphology of the deposited Au NPs, as shown in Figure 2c, is quite similar with that observed in Figure 2(a) (in the absence of SiO_2 NPs in preparation), but some aggregated SiO_2 NPs are coating on the deposited Au NPs. After the ORC treatment in 0.1 M KCl pH of solution is ca. 5.2, which is far higher than the IEP_{SiO2} of 2. Thus the produced $AuCl_4^-$ complexes can not be adsorbed on the postadded SiO_2 NPs due to the electrostatic repulsion for synthesizing Au/SiO_2 NCs with desired surface morphology after the following SEPD process. This phenomenon reminds us to notice the effect of the ORC treatment on the instantaneous adsorption of the produced positively charged Au ions in the anodic scans onto the surfaces of SiO_2 NPs besides the factor of difference between pH of solution and the IEP_{SiO2}. Encouragingly, as

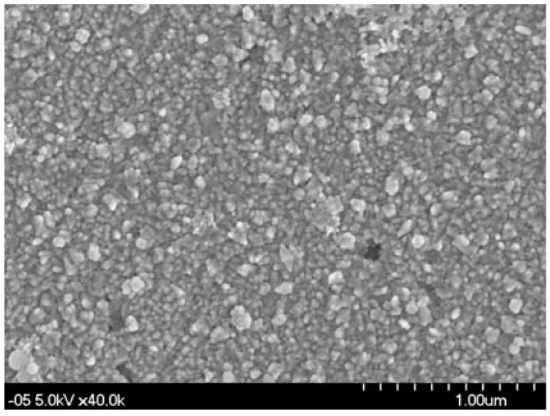

(a)

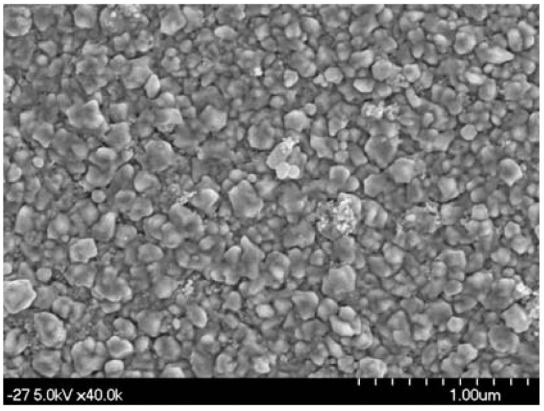

(b)

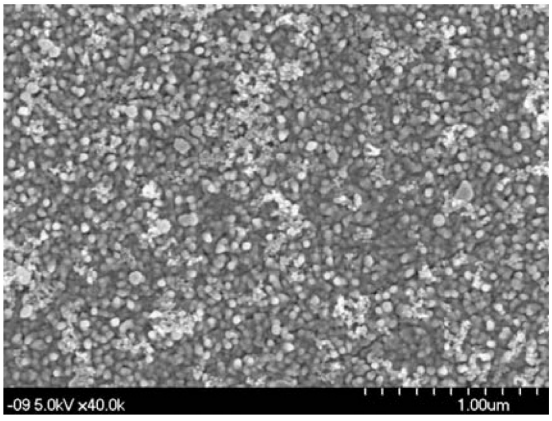

(c)

Figure 2. SEM images of different Au NP-deposited Pt substrates prepared in neutral solutions by using SEPD methods under a cathodic overpotential of 0.6 V and a rest overpotential of 0 V from OCP with a ratio of reaction times of pulse deposition of Au NPs to rest being 0.1: (a) Au NPs prepared in 0.1 M KCl; (b) Au/SiO_2 NCs prepared in 0.1 M KCl containing 1 mM SiO_2 NPs (addition before ORCs); (c) Au/SiO_2 NCs prepared in 0.1 M KCl containing 1 mM SiO_2 NPs (addition after ORCs).

shown in Figure 2b based on the Au/SiO_2 NCs prepared in 0.1 M KCl containing SiO_2 NPs before the ORC treatment, more closely packed and even Au NPs islands of ca. 70 nm with Raman activity can be observed. These Au NPs islands of ca. 70 nm can be clearly measured by magnifying this SEM image from the function of magnification attached in the software. Because molecules located between two metallic NPs display the greatest SERS enhancement[23,24] this kind of microstructure can provide more chances for probe molecules adsorbed on two metallic NPs. Therefore, a stronger SERS effect should be observed on this Au/SiO_2 NCs, as discussed later. Meanwhile, this bigger particle size of 70 nm is distinguishable from those of 40 nm based on other preparation conditions. As shown in the literature,[28] the SERS effect of Au NPs is also increased with an increase in the particle size of Au NPs in the range below 100 nm. Moreover, as shown in Figure 2b, there are significant amounts of edged Au NPs besides the spherical Au NPs deposited on substrates. These edged NPs should be more contributive to the total SERS effects than the spherical NPs are because the edged parts can induce enhanced instantaneously electromagnetic field under irradiation of laser light from the viewpoint of EM enhancement. This phenomenon was also observed in the study of SERS effects based on spherical and cube-like Au NPs, as shown in the literature.[29] We also tried to demonstrate the microstructure of the used SiO_2 NPs (see Figure S1in the Supporting Information). Because pure nonconductive SiO_2 NPs are difficultly deposited on the Pt substrate by using the SEPD method proposed in this work we demonstrate the SEM image of SiO_2 NPs by using the similar experimental method, which was employed for obtaining the surface morphology shown in Figure 1(b), but the used concentration of SiO_2 NPs is extremely high as 10 mM. In this image, SiO_2 NPs are the predominant components, as confirmed from the HRXPS analyses.

Then HRXPS analyses were performed to examine the surface components of Au/SiO_2 NCs and the corresponding oxidation states from the viewpoint of CHEM enhancement. Figure 3 displays the HRXPS Au spectra of the Au NPs prepared in 0.1 M HCl and 0.1 M KCl in the absence and presence of SiO_2 before and after ORC treatments. Basically,

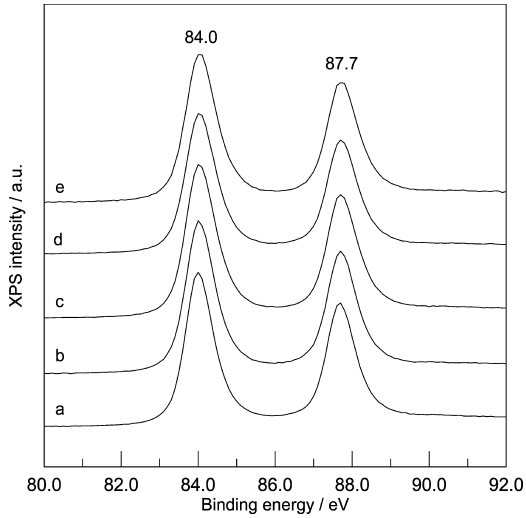

Figure 3. HRXPS Au $4f_{7/2-5/2}$ core-level spectra of different Au NPs-deposited Pt substrates prepared by using the same SEPD methods in different solutions: (a) in 0.1 M HCl; (b) in 0.1 M HCl containing 1 mM SiO_2 NPs (addition before ORCs); (c) in 0.1 M KCl; (d) in 0.1 M KCl containing 1 mM SiO_2 NPs (addition before ORCs); (e) in 0.1 M KCl containing 1 mM SiO_2 NPs (addition after ORCs).

dx.doi.org/10.1021/am3017366 | ACS Appl. Mater. Interfaces 2012, 4, 4700−4707

these five spectra are almost identical with the doublet peaks located at 84.0 and 87.7 eV, which can be assigned to Au(0).[30] It means that the Au in the Au NPs and Au/SiO_2 NCs deposited on substrates are all elemental states after the SEPD process. Detailed Si 2p spectra, as demonstrated in Figure 4,

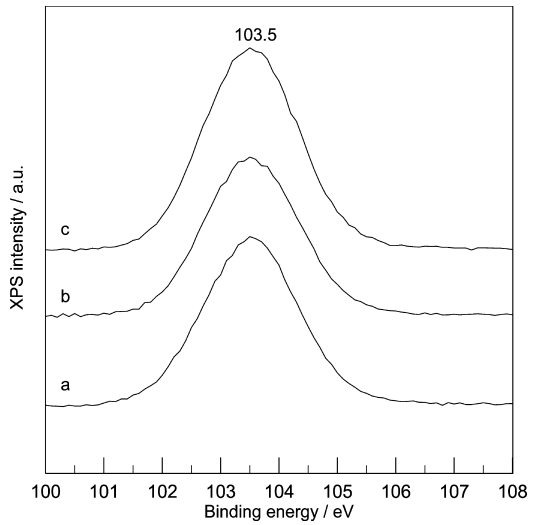

Figure 4. HRXPS Si 2p core-level spectra of different Au NPs-deposited Pt substrates prepared by using the same SEPD methods in different solutions: (a) in 0.1 M HCl containing 1 mM SiO_2 NPs (addition before ORCs); (b) in 0.1 M KCl containing 1 mM SiO_2 NPs (addition before ORCs); (c) in 0.1 M KCl containing 1 mM SiO_2 NPs (addition after ORCs).

were performed to examine the oxidation states of Si in the Au/SiO_2 NCs prepared in 0.1 M HCl and 0.1 M KCl in the presence of SiO_2 before and after ORC treatments. Basically, these three spectra are almost identical with the peaks located at 103.5 eV, which can be assigned to the oxidation state of Si^{4+} according to the XPS handbook and reports in the literature.[31,32] These results indicate that the oxidation state of Si in the Au/SiO_2 NCs is well-maintained during the formation of SERS-active Au/SiO_2 NCs deposited on substrates prepared by using SEPD methods proposed in this work. Moreover, the Au and SiO_2 composited in composition can be evaluated from further HRXPS analysis of surface chemical compositions based on their individual detailed spectra of Au and Si. The result shows that the content of SiO_2 is ca. 6.8 mol % (content of SiO_2 divided by contents of Au and SiO_2) for the prepared SiO_2-modified Au NCs (0.1 M KCl containing 1 mM SiO_2 NPs before ORC in preparation). This result can confirm that SiO_2 NPs were incorporated into the film Au NPs. Because pure SiO_2 NPs themselves are nonconductive they are difficultly evenly deposited on the Pt substrate by using the SEPD method. However, positively charged Au ions-adsorbed SiO_2 NPs are more easily evenly incorporated into the film of Au NPs with the electrodeposition of Au NPs by using the SEPD method.

As reported in the literature, it is believed that the SERS effect chiefly comes from the roughening procedure in ORC[33] and the corresponding complex formed at the interface of roughened metal.[21] Thus the complexes present in the Au/SiO_2 NCs prepared with different methods should be investigated to explicate the reasons for the correspondingly different SERS performances, as discussed later. Figure 5 displays the Cl 2p core-level spectra for Cl-containing complexes in the Au/SiO_2

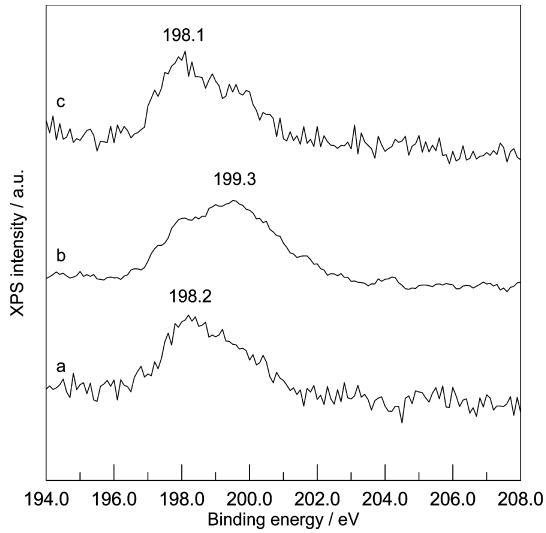

Figure 5. HRXPS Cl 2p core-level spectra of different Au NPs-deposited Pt substrates prepared by using the same SEPD methods in different solutions: (a) in 0.1 M HCl containing 1 mM SiO_2 NPs (addition before ORCs); (b) in 0.1 M KCl containing 1 mM SiO_2 NPs (addition before ORCs); (c) in 0.1 M KCl containing 1 mM SiO_2 NPs (addition after ORCs).

NCs prepared in 0.1 M HCl and 0.1 M KCl in the presence of SiO_2 before and after ORC treatments. These spectra indicate that the main peaks of the chloride-containing complexes present in the Au/SiO_2 NCs are located in the region between 196 and 203 eV. These chloride peaks can be approximately assigned to Cl (−1) according to the XPS handbook and a report in the literature.[34] When examining further, there are two different features that should be noticed. One is the oxidation state of Cl. The other is the content of Cl in the Au/SiO_2 NCs. As shown in Figure 5, the exactly main peaks are located at 198.2, 199.3, and 198.1 eV based on experiments performed in 0.1 M HCl with SiO_2 present before ORC, in 0.1 M KCl with SiO_2 present before ORC and in 0.1 M KCl with SiO_2 present after ORC, respectively. Obviously, the oxidation state of Cl in the Au/SiO_2 NCs prepared in 0.1 M KCl with SiO_2 present before ORC is higher than others. This phenomenon should be responsible for the higher SERS effect, as revealed from our previous reports.[35,36] Further composition analyses indicate that the contents of Cl in the Au/SiO_2 NCs are 4.8, 10.2, and 5.3 mol % for samples prepared in 0.1 M HCl with SiO_2 present before ORC, in 0.1 M KCl with SiO_2 present before ORC and in 0.1 M KCl with SiO2 present after ORC, respectively. These contents were determined from peak-area ratios of Cl to Cl, Au and Si in their corresponding detailed spectra corrected with the approximate instrument sensitivity factors. These phenomena of increased contents of Cl species are also contributive to their correspondingly increased SERS effects, as discussed later and shown in our previous report.[37]

SERS Performances of Au/SiO_2 NCs on Substrates. Figure 6 shows the Raman spectra of 2×10^{-6} M R6G adsorbed on the Au NPs and the Au/SiO_2 NCs prepared in 0.1 M HCl and 0.1 M KCl in the absence and presence of SiO_2 before and after ORC treatments. As demonstrated in spectrum a of Figure 6 based on Au NPs prepared in 0.1 M HCl without SiO_2 NPs, the SERS effect is the lowest one. Encouragingly, the SERS intensity of R6G observed on the Au/SiO_2 NCs prepared in 0.1 M KCl in the presence of SiO_2 before ORC treatment exhibits a higher relative intensity more than 1 order of

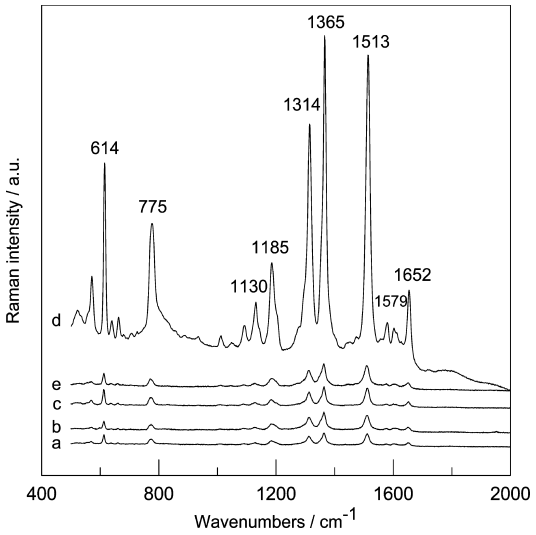

Figure 6. SERS spectra of 2×10^{-6} M R6G adsorbed on different Au NPs-deposited Pt substrates prepared by using the same SEPD methods in different solutions: (a) in 0.1 M HCl; (b) in 0.1 M HCl containing 1 mM SiO_2 NPs (addition before ORCs); (c) in 0.1 M KCl; (d) in 0.1 M KCl containing 1 mM SiO_2 NPs (addition before ORCs); (e) in 0.1 M KCl containing 1 mM SiO_2 NPs (addition after ORCs).

magnitude, as compared with those observed on the other four samples of Au NPs and the Au/SiO_2 NCs synthesized with other preparation conditions. This increase in intensity is significant in comparison with the reports of SERS spectra observed on various rough metal substrates.[38−40] In calculating the relative intensity, we employ the normalized Raman intensity, which is calculated from the ratio of the strongest intensity of R6G adsorbed on Au/SiO_2 NCs prepared in 0.1 M KCl in the presence of SiO_2 before ORC treatment to those of R6G adsorbed on the other four samples of Au NPs and the Au/SiO_2 NCs synthesized with other preparation conditions. Thus, no correction to the normal Raman scattering intensity is necessary to account for differences in sampling geometry and scattering phenomena.[41] As shown in spectrum d with the strongest SERS effect of Figure 6, it is characteristic of Raman spectrum of R6G.[42−44] The band at ca. 614 cm^{-1} is assigned to the C−C−C ring in-plane vibration mode. The band at ca. 774 cm^{-1} is assigned to the C−H out-of-plane bend mode. The bands at ca. 1130 and 1185 cm^{-1} are assigned to the C−H in-plane bend modes. The bands at ca. 1314 and 1579 cm^{-1} are assigned to the N−H in-plane bend modes. The bands at ca. 1365, 1510, and 1652 cm^{-1} are assigned to the C−C stretching modes. The EF value is calculated from the definition shown in the literature.[45] The EF per molecule is defined as $G = (N_2/N_1)/(I_{SERS}/I_{ref})$ where I_{SERS} is the integrated intensity of the R6G band under consideration recorded on the grating and I_{ref} is the integrated intensity of the same Raman band obtained by focusing the laser line on a Pt substrate immersed in a 2×10^{-3} M R6G solution. On the basis of this concentration of 2×10^{-3} M, the normal Raman spectroscopy of R6G is acceptable. N_1 is the number of molecules constituting the first monolayer adsorbed on the grating under the laser spot area. Because the real surface area of Au/SiO_2 NCs is difficultly obtained collection area based on laser spot size (2.5 μm^2) was used instead to calculate N_1 (collection area divided by the surface area of one R6G molecule). In the calculation, the surface area of one R6G molecule of 2×10^{-18} m^2/molecule was used.[46] This value was calculated from the geometric area of length (1.37 nm) × width (1.43 nm) of one R6G molecule. Thus, the estimated value for N_1 is ca. 1.25×10^6. N_2 is the number of molecules excited within the volume of the laser waist for the 2×10^{-3} M R6G solution. In calculating N_2 (irradiated solution volume multiplied by the concentration of analyzed molecule) the volume of the laser waist is approximately to a cylinder with a radius of 20 μm and a depth in the sample of 3 mm. The calculated volume is ca. 3.8×10^{-12} m^3. Thus, the estimated value for N_2 is ca. 4.5×10^{12}. On the basis of the ratio of (I_{SERS}/I_{ref}) being 1.5×10^2 calculated from the Raman intensities at ca. 1365 cm^{-1}, the prepared SERS-active substrate based on the optimum preparation condition demonstrates a large EF of 5.4×10^8. This obtained EF in this work is far higher than that of 1×10^6 observed on $Au@SiO_2$ core/shell structures[47] and even higher than that of 5.8×10^7 observed on Au NPs prepared by using our previously developed deposition−dissolution cycles.[15]

It is well-known that SiO_2 itself is a SERS-inactive material. In the SERS-active $Au@SiO_2$ core/shell structures, SiO_2 shell can prevent the core from interfering with the system under study.[17] In the SERS-active $SiO_2@Au$ core/shell structures, SiO_2 core can work as supports for the even growth of Au NPs.[18] In this work, it is quite interesting that the SERS effects observed on the Au/SiO_2 NCs based on the optimal preparation condition are markedly increased. The contributive factors have been well discussed before by using analyses of SEM and HRXPS from the viewpoints of EM and CHEM enhancements. Moreover, the SERS activity of SiO_2 NPs may come from the long-range effect of electromagnetic enhancement of adsorbed Au NPs, which is called the "borrowing SERS activity", as shown in the literature.[48,49]

To examine the sensitivity of the prepared SERS substrate, we analyzed different concentrations of R6G based on the Au/SiO_2 NCs-deposited Pt substrate, as shown in Figure 7. The linear correlation from 2×10^{-5} to 2×10^{-9} M with proportionality constant of unity indicates that the quantities of adsorption sites are large enough to accommodate considerable ranges of analyte concentrations.[50] Larger dynamical range of

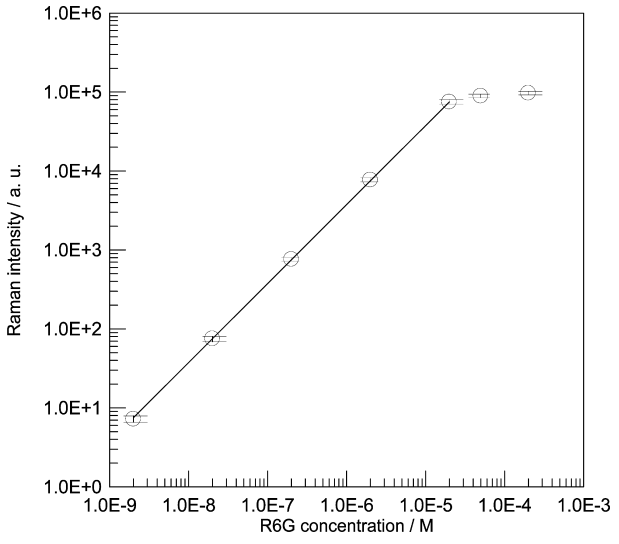

Figure 7. Raman intensities of R6G (at 1365 cm^{-1}) adsorbed on the Au/SiO_2 NCs (0.1 M KCl containing 1 mM SiO_2 NPs before ORC in preparation)-deposited Pt substrate as a function of R6G concentrations with logarithmic scales. The straight line is a guide to the eyes.

dx.doi.org/10.1021/am3017366 | ACS Appl. Mater. Interfaces 2012, 4, 4700−4707

more than 4 orders of magnitude observed on the Au/SiO_2 NC-deposited Pt substrate reveals that the developed SERS-active substrate is suitable for sensing chemical and biological molecules by SERS.

Meanwhile, as shown in the literature, Bell and Sirimuthu[51] suggested that the simplest way to reduce the error is to take multiple points on the surface of SERS-active solid substrates. Similarly, three measurements were used to evaluate the experimental errors in the study of SERS-active Ag films prepared from photoreduction of Ag ions on TiO_2.[52] Also, replicate measurements of six times on different areas were made to confirm the reproducibility of SERS substrate, as shown in the literature.[53] Based on the replicate measurements of five times on different areas and different batches of the as synthesized substrates were measured for three times (The relative deviations are all less than 5% in this work), and treatments for experimental errors shown in the literature, the uniformity and the repeatability of SERS substrates developed in this work are satisfactory.

Because the probe molecules of R6G have huge Raman cross sections the strategy proposed in this work to enhance SERS effects based on Au/SiO_2 NCs prepared by using SEPD methods was also applied on smaller probe molecules of 2,2′-bipyridine (BPy). Figure 8 shows the result of Raman spectrum

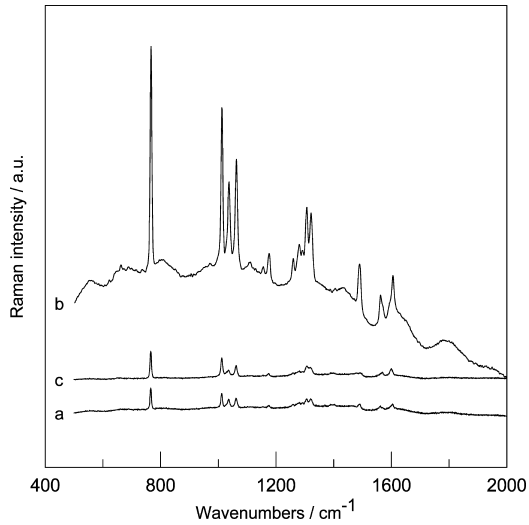

Figure 8. SERS spectra of 2×10^{-3} M 2,2′-bipyridine (BPy) adsorbed on different Au NPs-deposited Pt substrates prepared by using the same SEPD methods in different solutions: (a) in 0.1 M HCl containing 1 mM SiO_2 NPs (addition before ORCs); (b) in 0.1 M KCl containing 1 mM SiO_2 NPs (addition before ORCs); (c) in 0.1 M KCl containing 1 mM SiO_2 NPs (addition after ORCs).

of BPy adsorbed on the Au/SiO_2 NCs prepared in 0.1 M HCl and 0.1 M KCl in the presence of SiO_2 before and after ORC treatments. The bands shown in these spectra are characteristics of BPy on Raman spectrum.[54] The results also demonstrate similar phenomena. The SERS intensity of BPy observed on the Au/SiO_2 NCs prepared in 0.1 M KCl in the presence of SiO_2 before ORC treatment exhibits a higher relative intensity more than 1 order of magnitude, as compared with those observed on the Au/SiO_2 NCs prepared in 0.1 M HCl in the presence of SiO_2 before ORC treatment and on the Au/SiO_2 NCs prepared in 0.1 M KCl in the presence of SiO_2 after ORC treatment. Also, a simple analytical enhancement factor (AEF), which was defined as $(C_{ref}/C_{SERS})/(I_{SERS}/I_{ref})$,[55] was used to calculate the SERS enhancement factor. In this equation, C_{ref} (2 M) and C_{SERS} (2×10^{-3} M) represent the concentrations of BPy used for obtaining the I_{ref} and I_{SERS}, respectively, in measurements. The calculated value is ca. 8.5×10^7.

The influence of the degradations of Au/SiO_2 NCs-deposited and Au NPs-deposited Pt substrates on the corresponding SERS performance were also investigated in an atmosphere of 50% RH and 20% (v/v) O_2 at 30 °C for 4 weeks, as shown in Figure S2 in the Supporting Information. After 4 weeks, 93% of the relatively intensity still remained for the Au/SiO_2 NCs-deposited Pt substrate developed in this work. However, just 83% of the relative intensity remained for the unmodified Au NPs-deposited Pt substrate. In calculating the relative intensity, we employ the normalized Raman intensity, which is calculated from the ratio of the strongest band intensity of R6G at 1365 cm^{-1} adsorbed on the SERS-active substrate at any time to that of R6G adsorbed on the as-prepared SERS-active substrate. Accordingly, the proposed Au/SiO_2 NCs-deposited Pt substrate can significantly improve the SERS performance on antiaging ability.

CONCLUSIONS

In this work, a simple synthesis route based on SEPD methods has been successfully developed to synthesize effectively SERS-active Au/SiO_2 NCs with an enhancement factor of 5.4×10^8. The SERS intensities of typical probe molecules of R6G and small molecules of BPy adsorbed on the Au/SiO_2 NCs prepared in 0.1 M KCl in the presence of SiO_2 before ORC treatment exhibits a higher relative intensity more than 1 order of magnitude, as compared with those observed on the other four samples of Au NPs and the Au/SiO_2 NCs synthesized with other preparation conditions. From the viewpoint of EM enhancement to explain these phenomena the synthesized Au/SiO_2 NCs deposited on substrates based on optimal preparation condition demonstrate more closely packed and even Au NPs islands with bigger particle sizes of 70 nm and more edged particles. Also, the content and the oxidation state of Cl in these Au/SiO_2 NCs are higher, which are contributive to the SERS effects from the viewpoint of CHEM enhancement.

ASSOCIATED CONTENT

Supporting Information

SEM image of SiO_2 NPs and variation of SERS effect in aging test. This information is available free of charge via the Internet at http://pubs.acs.org/.

AUTHOR INFORMATION

Corresponding Author

*Tel.: 886-2-27361661, ext 3155. Fax: 886-2-27356689. E-mail: liuyc@tmu.edu.tw.

Notes

The authors declare no competing financial interest.

ACKNOWLEDGMENTS

The authors thank the National Science Council of the Republic of China and Taipei Medical University for their financial support.

REFERENCES

(1) Vijayan, B. K.; Dimitrijevic, N. M.; Finkelstein-Shapiro, D.; Wu, J.; Gray, K. A. *ACS Catal.* **2012**, *2*, 223−229.
(2) Zimny, K.; Roques-Carmes, T.; Carteret, C.; Stébé, M. J.; Blin, J. L. *J. Phys. Chem. C* **2012**, *116*, 6585−6594.
(3) Kalbac, M.; Farhat, H.; Kong, J.; Janda, P.; Kavan, L.; Dresselhaus, M. S. *Nano Lett.* **2011**, *11*, 1957−1963.
(4) Pinkhasova, P.; Yang, L.; Zhang, Y; Sukhishvili, S. A.; Du, H. *Langmuir* **2012**, *28*, 2529−2535.
(5) Mosier-Boss, P. A.; Lieberman, S. H. *Langmuir* **2003**, *19*, 6826−6836.
(6) Jeong, D. H.; Zhang, Y. X.; Moskovits, M. *J. Phys. Chem. B* **2004**, *108*, 12724−12728.
(7) Liu, Y. C.; Yang, K. H.; Hsu, T. C. *Anal. Chim. Acta* **2009**, *636*, 13−18.
(8) Tognalli, N. G.; Cortés, E.; Hernández-Nieves, A. D.; Carro, P.; Usaj, G.; Balseiro, C. A.; Vela, M. E.; Salvarezza, R. C.; Fainstein, A. *ACS Nano* **2011**, *5*, 5433−5443.
(9) Wang, H. H.; Liu, C. Y.; Wu, S. B.; Liu, N. W.; Peng, C. Y.; Chan, T. H.; Hsu, C. F.; Wang, J. K.; Wang, Y. L. *Adv. Mater.* **2006**, *18*, 491−495.
(10) Zhu, C.; Meng, G.; Huang, Q.; Huang, Z.; Chu, Z. *Cryst. Growth Des.* **2011**, *11*, 748−752.
(11) Liao, Q.; Mu, C.; Xu, D. S.; Ai, X. C.; Yao, J. N.; Zhang, J. P. *Langmuir* **2009**, *25*, 4708−4714.
(12) Pemberton, J. E.; Guy, A. L.; Sobocinski, R. L.; Tuschel, D. D.; Cross, N. A. *Appl. Surf. Sci.* **1988**, *32*, 33−41.
(13) Grasselli, J. G.; Bulkin, B. J. *Analytical Raman Spectroscopy*; John Wiley & Sons: New York, 1991; pp 295−298.
(14) Yang, K. H.; Liu, Y. C.; Yu, C. C.; Chen, B. C. *J. Phys. Chem. C* **2010**, *114*, 12863−12869.
(15) Mai, F. D.; Hsu, T. C.; Liu, Y. C.; Yang, K. H.; Chen, B. C. *Chem. Commun.* **2011**, *47*, 2958−2960.
(16) Mubeen, S.; Zhang, S.; Kim, N.; Lee, S.; Krämer, S.; Xu, H.; Moskovits, M. *Nano Lett.* **2012**, *12*, 2088−2094.
(17) Li, J. F.; Huang, Y. F.; Ding, Y.; Yang, Z. L.; Li, S. B.; Zhou, X. S.; Fan, F. R.; Zhang, W.; Zhou, Z. Y.; Wu, D. Y.; Ren, B.; Wang, Z. L.; Tian, Z. Q. *Nature* **2010**, *464*, 392−395.
(18) Zeng, J.; Jean, D.; Ji, C.; Zou, S. *Langmuir* **2012**, *28*, 957−964.
(19) Gerein, N. J.; Haber, J. A. *J. Phys. Chem. B* **2005**, *109*, 17372−17385.
(20) Seney, C. S.; Gutzman, B. M.; Goddard, R. H. *J. Phys. Chem. C* **2009**, *113*, 74−80.
(21) Baibarac, M.; Mihut, L.; Louarn, G.; Mevellec, J. Y.; Wery, J.; Lefrant, S.; Baltog, I. *J. Raman Spectrosc.* **1999**, *30*, 1105−1113.
(22) Liu, Y. C. *Langmuir* **2002**, *18*, 174−181.
(23) Liver, N.; Nitzan, A.; Gersten, J. *Chem. Phys. Lett.* **1984**, *111*, 449−454.
(24) Xu, M.; Dignam, M. J. *J. Chem. Phys.* **1994**, *100*, 197−203.
(25) Jang, J.; Ha, J.; Lim, B. *Chem. Commun.* **2006**, 1622−1624.
(26) Dawson, A.; Kamat, P. V. *J. Phys. Chem. B* **2001**, *105*, 960−966.
(27) Cardini, G.; Maurizio-Miranda, M.; Schettino, V. *J. Phys. Chem. B* **2004**, *108*, 17007−17011.
(28) Hu, J. W.; Li, J. F.; Ren, B.; Wu, D. Y.; Sun, S. G.; Tian, Z. Q. *J. Phys. Chem. C* **2007**, *111*, 1105−1112.
(29) Narayanan, R.; Lipert, R. J.; Porter, M. D. *Anal. Chem.* **2008**, *80*, 2265−2271.
(30) Henry, M. C.; Hsueh, C. C.; Timko, B. P.; Freund, M. S. *J. Electrochem. Soc.* **2001**, *148*, D155−161.
(31) He, P.; Hu, N.; Rusling, J. F. *Langmuir* **2004**, *20*, 722−729.
(32) Kim, Y. H.; Lee, D. K.; Cha, H. G.; Kim, C. W.; Kang, Y. S. *J. Phys. Chem. C* **2007**, *111*, 3629−3635.
(33) Pockrand, I. *Chem. Phys. Lett.* **1982**, *85*, 37−40.
(34) Schmeisser, D.; Naaemann, H.; Gopel, W. *Synth. Met.* **1993**, *59*, 211−221.
(35) Liu, Y. C. *Langmuir* **2002**, *18*, 174−181.
(36) Yang, K. H.; Liu, Y. C.; Yu, C. C. *Electrochim. Acta* **2009**, *54*, 4202−4207.
(37) Yang, K. H.; Liu, Y. C.; Yu, C. C. *Langmuir* **2010**, *26*, 11512−11517.
(38) Wang, C. C. *J. Phys. Chem. C* **2008**, *112*, 5573−5578.
(39) Liu, Y. C.; Lin, P. I.; Chen, Y. T.; Ger, M. D.; Lan, K. L.; Lin, C. L. *J. Phys. Chem. B* **2004**, *108*, 14897−14900.
(40) Baibarac, M.; Cochet, M.; Lapkowski, M.; Mihut, L.; Lefrant, S.; Baltog, I. *Synth. Met.* **1998**, *96*, 63−70.
(41) Taylor, C. E.; Pemberton, J. E.; Goodman, G. G.; Schoenfisch, M. H. *Appl. Spectrosc.* **1999**, *53*, 1212−1221.
(42) Lu, Y.; Liu, G. L.; Lee, L. P. *Nano Lett.* **2005**, *5*, 5−9.
(43) Sun, Z.; Li, Y.; Wang, Y.; Chen, X.; Zhang, J.; Zhang, K.; Wang, Z.; Bao, C.; Zeng, J.; Zhao, B.; Yang, B. *Langmuir* **2007**, *23*, 10725−10731.
(44) Jensen, L.; Schatz, G. C. *J. Phys. Chem. A* **2006**, *110*, 5973−5977.
(45) Felidj, N.; Aubard, J.; Levi, G.; Krenn, J. R.; Salerno, M.; Schider, G.; Lamprecht, B.; Leitner, A.; Aussenegg, F. R. *Phys. Rev. B* **2002**, *65*, 075419.
(46) Tsurumachi, N.; Okamoto, H.; Ishii, K.; Kohkami, H.; Nakanishi, S.; Ishii, T.; Takahashi, N.; Dou, C.; Wen, P.; Feng, Q. *J. Photoch. Photobio. A* **2012**, *243*, 1−6.
(47) Li, J.; Ding, S.; Yang, Z.; Bai, M.; Anema, J. R.; Wang, X.; Wang, A.; Wu, D.; Ren, B.; Hou, S.; Wandlowski, T.; Tian, Z. *J. Am. Chem. Soc.* **2011**, *133*, 15922−15925.
(48) Song, W.; Wang, Y.; Zhao, B. *J. Phys. Chem. C* **2007**, *111*, 12786−12791.
(49) Zwijnenburg, A.; Goossens, A.; Sloof, W. G.; Craje, M. W. J.; Kraan, A. M.; Jongh, L. J.; Makkee, M.; Moulijn, J. A. *J. Phys. Chem. B* **2002**, *106*, 9853−9862.
(50) Wang, H. H.; Liu, C. Y.; Wu, S. B.; Liu, N. W.; Peng, C. Y.; Chan, T. H.; Hsu, C. F.; Wang, J. K.; Wang, Y. L. *Adv. Mater.* **2006**, *18*, 491−494.
(51) Bell, S. E. J.; Sirimuthu, N. M. S. *Chem. Soc. Rev.* **2008**, *37*, 1012−1024.
(52) Sudnik, L. M.; Norrod, K. L.; Rowlen, K. L. *Appl. Spectrosc.* **1996**, *50*, 422−424.
(53) Xia, W.; Sha, J.; Fang, Y.; Lu, R.; Luo, Y.; Wang, Y. *Langmuir* **2012**, *28*, 5444−5449.
(54) Wang, C. C.; Chen, J. S. *Electrochim. Acta* **2008**, *53*, 5615−5620.
(55) Le Ru, E. C.; Blackie, E.; Meyer, M.; Etchegoin, P. G. *J. Phys. Chem. C* **2007**, *111*, 13794−13803.